

Theoretical chemistry of α -graphyne: functionalization, symmetry breaking, and generation of Dirac-fermion mass

R. Longuinhas¹, E. A. Moujaes², S. S. Alexandre¹, and R. W. Nunes¹

¹*Departamento de Física, ICEx, Universidade Federal de Minas Gerais, 31270-901, Belo Horizonte, MG, Brazil*

²*Departamento de Física, Universidade Federal de Rondônia, 76900-900, Porto Velho, Brazil*

(Dated: April 2, 2014)

We investigate the electronic structure and lattice stability of pristine and functionalized (with either hydrogen or oxygen) α -graphyne systems. We identify lattice instabilities due to soft-phonon modes, and describe two mechanisms leading to gap opening in the Dirac-fermion electronic spectrum of these systems: symmetry breaking, connected with the lattice instabilities, and partial incorporation of an sp^3 -hybrid character in the covalent-bonding network of a buckled hydrogenated α -graphyne lattice that retains the symmetries of the parent pristine α -graphyne. In the case of an oxygen-functionalized α -graphyne structure, each O atom binds asymmetrically to two twofold-coordinated C atoms, breaking inversion and mirror symmetries, and leading to the opening of a sizeable gap of 0.22 eV at the Dirac point. Generally, mirror symmetries are found to suffice for the occurrence of gapless Dirac cones in these α -graphyne systems, even in the absence of inversion symmetry centers. Moreover, we analyze the gapless and gapped Dirac cones of pristine and functionalized α -graphynes from the perspective of the dispersion relations for massless and massive free Dirac fermions. We find that mirror-symmetry breaking mimics a Dirac-fermion mass-generation mechanism in the oxygen-functionalized α -graphyne, leading to gap opening and to isotropic electronic dispersions with a rather small electron-hole asymmetry. In the hydrogen-functionalized case, we find that carriers show a remarkable anisotropy, behaving as massless fermions along the **M-K** line in the Brillouin zone and as massive fermions along the **Γ -K** line.

PACS numbers:

I. INTRODUCTION

Monolayer and few-layer graphene have been under intensive scientific scrutiny since their isolation and identification on a variety of substrates^{1–3} This research effort has also generated an increasing interest in the identification of other two-dimensional (2D) materials that could possibly share the linear dispersion and chiral nature of the electronic carriers in graphene, along with the ensuing exceptional electronic properties.^{4–6} Topological insulators,⁷ silicene,⁸ monolayer boron-nitride,⁹ and monolayers of inorganic layered materials such as molybdenum sulfide¹⁰, have since come into the fold.

Nevertheless, the all-carbon “sector” of this problem has not been fully exhausted, and families of two-dimensional (2D) carbon allotropes named graphynes have also been investigated for the occurrence of Dirac cones of electronic states.^{11,12} While synthesis of crystalline forms of graphynes is still lacking, many chemical routes have been reported for the large molecules that form the building blocks for such crystals^{13–15}. A few recent works have examined these graphyne systems, related hydrocarbons, and other functionalized forms.^{16,17} Further in-depth theoretical investigation of the electronic properties and lattice stability of such carbon allotropes is a crucial step in gauging the potential applications of graphynes as graphene-like materials.

Among a variety of possible graphyne lattices^{11,12,18}, the so-called α -graphyne (α Gy) shares with graphene the hexagonal Bravais lattice and the presence of two threefold-coordinated carbon atoms that occupy the sites of a 2D honeycomb lattice. In α Gy, the threefold carbons

are connected by linear chains of two twofold-coordinated carbon atoms, as shown in Fig. 1(a). Linear chains with a different number of twofold carbon atoms connecting the threefold honeycomb sites are also conceivable. Figure 1(b) shows the case of one-atom chains.

In any α Gy lattice, for any length of the twofold-carbon chains, an inversion-symmetry center in the middle of any given linear chain relates the twofold-coordinated atoms two-by-two (except for one carbon atom that sits at the inversion center in odd-membered chains) and the two threefold sites are inversion-symmetry partners as well. From this perspective, inversion symmetry could be believed to be a requirement for the occurrence of Dirac cones in the electronic dispersion of α -graphynes, as in graphene. This question was touched upon in Ref. 12, where it was shown by explicit calculations for the so-called 6,6,12-graphyne that a lattice need not belong to the $p6m$ hexagonal-symmetry group to display Dirac cones in its electronic dispersion. The 6,6,12-graphyne lattice belongs to the pmm rectangular symmetry group, yet Dirac cones appear in its electronic structure, albeit not at the **K**-point in the Brillouin zone (BZ).¹² Given that both of these lattice-symmetry groups display twofold-symmetry axes (which are equivalent to inversion centers in 2D lattices), the question of whether inversion symmetry is a requirement for the occurrence of Dirac cones still stands.

In this work, we examine the nature of the electronic states of planar α -graphynes with linear chains of one [α Gy1 in Fig. 1(b)] and two [α Gy2 in Fig. 1(a)] twofold carbon atoms, and discuss the chemical-bond picture that determines the chemical stabilization of these car-

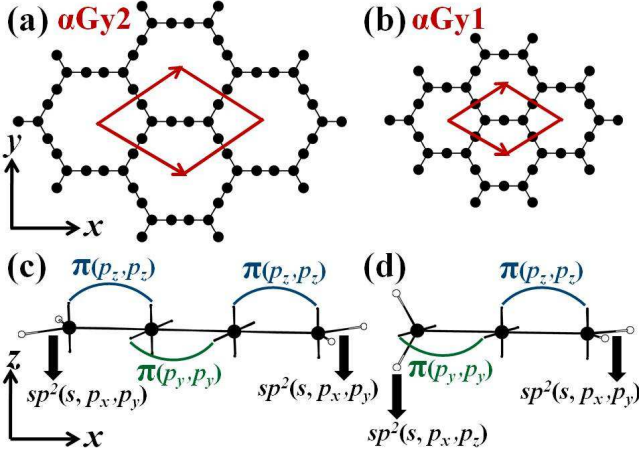


FIG. 1: α -graphyne (α Gy) 2D lattices and corresponding linear molecular forms. (a) α Gy2 with two twofold carbon atoms in the linear chains connecting the threefold sites. Lattice vectors and the eight-atom primitive cell are indicated. (b) α Gy1 with one twofold carbon atom in the linear chains. Lattice vectors and the five-atom primitive cell are indicated. (c) Butatriene: C_4H_4 hydrocarbon with co-planar methylene (CH_2) groups at the edges. (d) Allene: C_3H_4 hydrocarbon with perpendicular methylene groups at the edges. In (c) and (d), the π -bonding scheme along the chains and the sp^2 bonding of the methylene groups are indicated.

bon allotropes by the saturation of in-plane p orbitals, promoted by covalent binding of either hydrogen or oxygen with the twofold carbons along the chains, yielding: (i) an α Gy2-based hydrocarbon showing Dirac cones of electronic states at the Fermi energy (E_f); and (ii) an α Gy2-based graphyne oxide that meets the oft-quoted need of the presence of a gap in the electronic dispersion at the Fermi level.

Furthermore, we investigate the lattice stability of graphyne hydrocarbons based on both α Gy1 and α Gy2, aiming at identifying possible lattice instabilities of the 2D geometries and their impact on the electronic dispersions of these systems. We also examine symmetry requirements for the presence of Dirac cones of massless fermions in the electronic spectrum of these systems, as well as the connection between symmetry breaking and the presence of gaps, or lack thereof, in the Dirac-cone spectrum of pristine and functionalized α Gy1 and α Gy2. We describe two different mechanisms for gap opening in the Dirac cones of α -graphyne systems: (i) symmetry breaking; (ii) incorporation of an sp^3 -hybrid content in the covalent-bonding network of the twofold C atoms.

We find that while a pristine 2D α Gy2 lattice is fully stable, with no soft modes in the phonon spectrum, a planar form of an α Gy2+H hydrocarbon, with C_8H_6 stoichiometry, shows a soft-phonon mode at the Γ point in the phonon BZ that drives the system to a fully stable (no soft-phonon modes) buckled geometry, with off-plane displacements of the twofold carbons and the saturating

hydrogen atoms, as shown in Fig. 2(b). The soft-mode displacements preserve the inversion centers and mirror symmetries of the planar α Gy2+H lattice, yet we observe the opening of a gap of ~ 0.05 eV in the Dirac cone at E_f , which is related to the partial incorporation of an sp^3 character in the covalent bonds of the twofold C atoms. The gapped Dirac cone at E_f in the buckled α Gy2+H lattice is strongly anisotropic, with a linear dispersion (hence massless fermions) along the M - K direction in the BZ and a quadratic dispersion (hence massive fermions) along the K - Γ direction.

In the case of the planar α Gy2+O system with C_8O_3 stoichiometry, each O atom binds asymmetrically to the two twofold C atoms in the chains, as shown in Fig. 2(c), breaking both inversion and mirror symmetries and leading to the opening of a sizeable gap of 0.22 eV in the Dirac cone at E_f .

In the case of α Gy1, the pristine planar α Gy1 lattice is found to be chemically unstable, due to the formation of in-plane π bonds that leads to frustration of the planar geometry. Saturation of in plane p orbitals, by hydrogen functionalization, inhibits the formation of the destabilizing π bonds, and produces a planar α Gy1+H geometry (C_5H_3 stoichiometry) that lacks inversion symmetry but keeps the mirror planes cutting the lattice plane through the CH bonds. The mirror planes are found to suffice for the occurrence of gapless Dirac cones in the electronic structure of this 2D α Gy1+H geometry. Moreover, this planar geometry shows a lattice instability, due to a soft-phonon mode at the Γ point, leading to a buckled structure with off-plane displacements of twofold carbons and hydrogen atoms, as shown in Fig. 2(a). Mirror-symmetry breaking, connected with the soft-mode displacements, leads to gap openings ranging from 0.16 to 0.60 eV at the Dirac points in the electronic spectrum of this system.

Furthermore, we analyze gapless and gapped Dirac cones of the α Gy2, α Gy2+H, and α Gy2+O systems, from the perspective of the dispersion relations for massless and massive free Dirac fermions. We find that the electronic bands of the gapped α Gy2+O system are isotropic, display a small (~ 5 -6%) electron-hole asymmetry, and are very well described by the relativistic energy-momentum dispersion relation for free massive Dirac fermions, suggesting that symmetry breaking operates as a mechanism of mass generation for the Dirac charge carriers in α Gy2+O. In the case of the buckled α Gy2+H system, we find a strongly anisotropic behavior, with carriers acting as massless fermions along the M - K line in the BZ and as massive fermions along the Γ - K line. Moreover, effective hopping values in α -graphynes are computed by employing the standard relations between hopping integrals, M -point van Hove-singularity gaps, and Fermi velocities obtained from the standard tight-binding description of graphene, in order to explain the reduction of carrier velocities in α -graphynes, when compared with graphene.

II. METHODS

The electronic structure analysis and structural optimization of the α Gy systems were carried out using the SIESTA code¹⁹. Geometry relaxation was performed until the total force on each atom was lower than 4×10^{-2} eV/Å, and pressures were lower than 0.5 Kbar. We used a $64 \times 64 \times 1$ Monkhorst-Pack (MP)²⁰ \mathbf{k} -point sampling of the BZ, and an atomic basis set with two polarization zeta functions (DZP), with an energy shift of 0.01 Ry and a mesh cutoff of 250 Ry. Trouiller-Martins norm-conserving pseudopotentials in the fully non-local scheme were employed for the interaction between valence electrons and ionic cores^{21,22}. The SIESTA calculations were performed using a van der Waals functional (vdW-DF)^{23,24} and double checked with the PBE GGA functional²⁵. The two functionals lead to similar results, as expected for these systems.

The study of lattice stability was performed within the density functional perturbation theory²⁶, as implemented in the Quantum Espresso (QE) code²⁷. In these calculations we further relaxed the Siesta-relaxed structures until the forces were lower than 2×10^{-3} eV/Å and the pressure was lower than 0.5 Kbar. A plane-wave energy cutoff of 32 Ry was found to produce well-converged results. Ionic cores were represented by ultrasoft pseudopotentials^{28,29}. We used the PBE GGA functional²⁵ and double checked the calculations for negative frequencies using the LDA functional. The Fermi surface was smeared using cold smearing³⁰ with a degauss of 0.01. We used a \mathbf{k} -point sampling grid of $12 \times 12 \times 1$ for the electronic states and a \mathbf{q} -point sampling grid of $4 \times 4 \times 1$ for the phonon calculations. The threshold for the calculations of phonon spectra was 10^{-21} .

III. RESULTS AND DISCUSSION

A. Chemical-bond constraints on the stability of planar α -graphynes

We start by outlining chemical considerations indicating that pristine α -graphynes with odd numbers of twofold carbon atoms along the chains should be unstable in the planar form, due to chemical frustration. This can be understood by considering the sp -hybrid covalent bonding of the following molecular hydrocarbons known as cumulenes: butatriene (C_4H_4) and hexapentaene (C_6H_4), that are stable in a planar form, and allene (C_3H_4) and pentatetraene (C_5H_4), with an extended-tetrahedral structure where the methylene groups at the two terminations of the molecule are perpendicular to each other^{31,32}. For the sake of the argument, it suffices to consider butatriene and allene, shown in Figs. 1(c) and (d), respectively.

In Figs. 1(c) and (d), the axis of each molecule lies

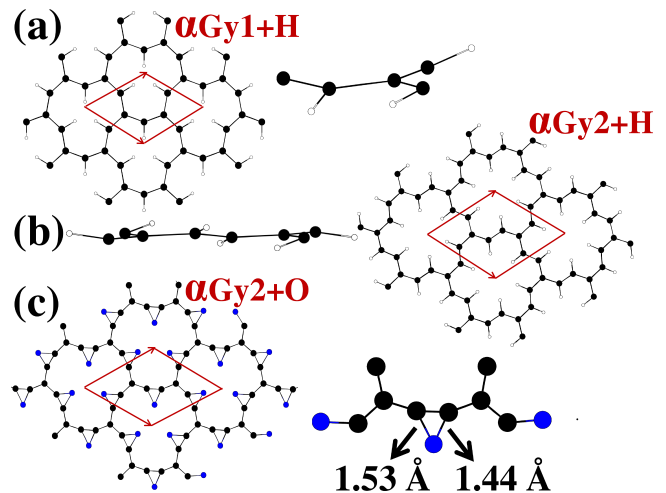


FIG. 2: Functionalized α -graphyne structures. (a) Left side: top view of planar α Gy1+H; lattice vectors and the primitive cell with C_5H_3 stoichiometry are indicated. Right side: lateral view of the C_5H_3 unit of the buckled geometry, showing asymmetric off-plane displacements of C and H atoms. (b) Right side: top view of planar α Gy2+H; lattice vectors and the primitive cell with C_8H_6 stoichiometry are indicated. Left side: lateral view of the C_8H_6 unit of the buckled geometry, showing symmetric off-plane displacements of C and H atoms. (c) Left side: top view of planar α Gy2+O; lattice vectors and the primitive cell with C_8O_3 stoichiometry are indicated. Right side: planar C_8O_3 unit showing asymmetric bonding of the O atom with the two C atoms in the linear chain. C, O, and H atoms are shown as black, blue, and white circles, respectively.

along the x direction, and the twofold atoms in the chain form σ bonds along the chain axis, involving sp_x hybrids. In the case of allene in Fig. 1(d), with a single twofold carbon atom connecting the threefold carbons at each end of the molecule, the plane formed by the methylene group (CH_2) on the left end must be perpendicular to that on the right end of the molecule. This follows from the fact that whenever the covalent double bond between the twofold C atom and the threefold one on the right involves a π bond between p_z orbitals, the double bond with the threefold atom on the left must necessarily involve a π bond between the p_y orbitals of the two atoms. This means that when CH bonds on the right are (s, p_x, p_y) sp^2 hybrids, those on the left must be (s, p_x, p_z) sp^2 hybrids, as illustrated in Fig. 1(d), leading to the chemical frustration of the planar form. This is true for any odd number of atoms in the chain connecting the two threefold carbons. For even-membered chains, a similar argument shows that the methylene groups at the two ends lie on the same plane, as shown in Fig. 1(c). This translates into chemical-bond constraints on the stability of extended geometries: stable planar forms are not expected for odd-membered chains.

The α Gy1 and α Gy2 lattices are the extended analogs of allene and butatriene, respectively. We performed an *ab initio* structural optimization of the α Gy1 system,

starting from a fully planar geometry, that resulted in a highly distorted structure, due to chemical frustration, while αGy2 retained a 2D form and the honeycomb lattice upon structural relaxation, providing confirmation of the above chemical-bond picture. Throughout this report, we address the lattice stability of the hydrogen-functionalized αGy systems we propose. The lattice stability of pristine αGy2 has been addressed in Ref³³, with no unstable phonon modes found in this system, a result that we have confirmed in our calculations.

The bond chemistry outlined in Figs 1(c) and (d) also suggests that in-plane functionalization of α -graphynes should lead to stabilization of planar forms, at least from the perspective of the chemical saturation of the in-plane p orbitals of the twofold carbons in the chains. Below, we consider in-plane functionalization with either hydrogen or oxygen, and address the electronic structure and lattice stability of the planar forms.

B. Electronic structure of pristine α -graphyne

Let us first consider the nature of the electronic bands and the corresponding density of states (DOS) of the pristine αGy2 structure, as shown in Fig. 3. In the figure, we also show the partial density of states (PDOS) for the twofold and threefold C atoms. We consider αGy2 monolayers on the xy plane as in Figs. 1(a) and (b). The remarkable similarity of the αGy2 electronic structure with that of graphene itself has been pointed out in recent works^{12,34,35}. Here, we take a closer look at the αGy2 electronic dispersion and discuss where it differs from that of graphene.

In graphene, the two p_z orbitals per unit cell give rise to the two π bands crossing each other at E_f . In αGy2 , there are eight C atoms per unit cell, and we expect eight bands connected with the eight p_z orbitals in the cell. Regarding the Dirac cone at E_f in Fig. 3, altogether the orbitals of the six twofold atoms account for $\sim 65\text{--}70\%$ of the related DOS, and the two threefold C atoms contribute the remaining $\sim 30\text{--}35\%$, showing that the p_z orbitals of the twofold C atoms resonate with the p_z orbitals of the threefold C atoms to form the metallic π band. This clearly indicates that the presence of an inversion symmetry center in the middle of the twofold-carbon chain and an underlying hexagonal-symmetry lattice enable the appearance of Dirac cones of resonating π orbitals even for the more complex atomic basis of αGy2 , when compared with graphene.

Figure 3 also shows additional Dirac cones with the same overall band topology as the one at E_f , one with its Dirac point at ~ 5.0 eV below E_f , with nearly the same orbital composition, and another at ~ 5.0 eV above E_f , the latter being derived from linear combinations of the in-plane (p_x and p_y) orbitals which are perpendicular to the twofold-carbon chains. Moreover, strongly localized

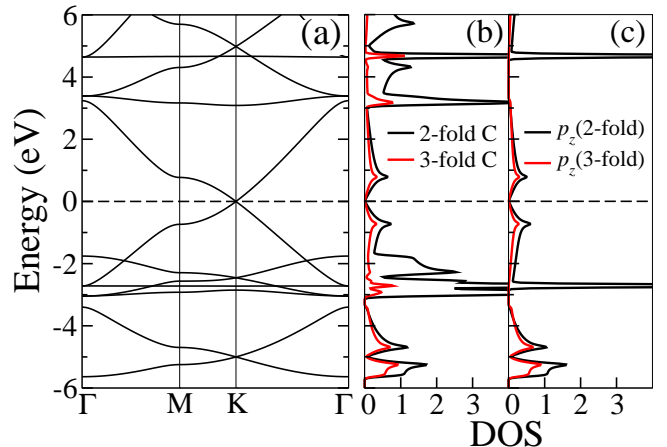


FIG. 3: (a) Band structure of pristine αGy2 along the Γ -M, M-K, and M- Γ high-symmetry lines in the Brillouin zone. (b) Black line: partial density of states (PDOS) projected on all basis orbitals of the six twofold C atoms. Red line: PDOS projected on all orbitals of the two twofold C atoms. (c) Black line: PDOS projected on the p_z orbitals of the six twofold C atoms. Red line: PDOS projected on the p_z orbitals of the two twofold C atoms.

molecular-like bonding and antibonding combinations of these in-plane p orbitals of the twofold C atoms are also observed, as indicated by the nearly dispersionless bands that appear as sharp Dirac-delta-like peaks in the DOS, at ~ 3.3 eV above and ~ 3.0 eV below E_f . These localized states have no p_z orbital character, as shown by the PDOS curves in Figs. 3(b) and (c). Localized states derived from the p_z orbitals also appear as two flat bands one at ~ 2.7 eV below and another at ~ 4.6 eV above E_f [Figs. 3(b) and (c)].

C. Hydrogen functionalization of α -graphyne: electronic structure and lattice stability

The above chemical-bond and electronic-structure analysis suggests possible ways of adding other atomic species such as hydrogen or oxygen in order to form stable αGy2 compounds. The in-plane p orbitals are natural candidates to form CH bonds with H atoms added in the plane, in the voids of the αGy2 lattice. The localized character of the molecular-like states derived from these in-plane orbitals suggests a strong reactivity to functional groups. In the case of αGy1 , bond chemistry suggests that the chemical frustration of the planar structure observed in the pristine αGy1 lattice should be suppressed by passivating the in-plane p orbitals, thus inhibiting the formation of the destabilizing π bonds from these orbitals.

Indeed, *ab initio* structural relaxation of a $\alpha\text{Gy1}+\text{H}$ hydrocarbon (C_5H_3 stoichiometry), where in-plane H

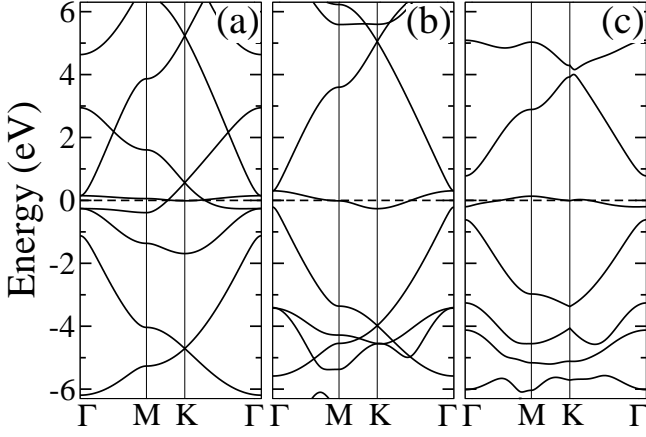


FIG. 4: (a) Band structure of a constrained (see text) planar pristine αGy1 lattice along high-symmetry lines in the Brillouin zone. (b) Band structure of a planar functionalized $\alpha\text{Gy1+H}$ lattice. (c) Band structure of a buckled functionalized $\alpha\text{Gy1+H}$ lattice showing gap openings on the Dirac cones at the \mathbf{K} -point.

atoms bond to the twofold C atoms in the chains, leads to the planar structure shown in Fig. 2(a). To be precise, in our calculations the planar $\alpha\text{Gy1+H}$ is “numerically stable”, in the sense that starting from an initial planar geometry where all C and H atoms lie on the xy plane, the structure relaxes into a planar geometry that retains the honeycomb-like lattice and shows Dirac cones in its electronic structure, as displayed in Fig. 4(b). Note, however, that no Dirac cone is found at E_f , where we observe only a band with a small dispersion, connected with localized states derived from the p_z orbitals of the twofold C atoms. This nearly dispersionless band at E_f is likely a feature of the electronic structure of any odd-membered αGy lattice.

For comparison, Fig. 4(a) shows the electronic bands for a pristine αGy1 geometry (without H atoms) that was constrained to remain in the planar hexagonal lattice, where we also observe the band of localized states crossing the Fermi level, and the occurrence of Dirac cones at the \mathbf{K} -point, in energies above and below E_f . In this case, we observe a cone with its Dirac point at ~ 0.5 eV above E_f and a dispersive band just below E_f , both composed nearly entirely of the p_x and p_y orbitals of the twofold C atoms. Upon hydrogen saturation of the in-plane p orbitals, these bands are shifted away from the Fermi level, as shown in Fig. 4(b).

The picture drawn above of the chemical stability of the planar $\alpha\text{Gy1+H}$ provides only a heuristic argument, and does not exclude the possibility of lattice instabilities due to soft-phonon modes in the phonon dispersion relation for this structure. In order to address this issue, we computed the phonon frequencies at the Γ point in the BZ for the planar $\alpha\text{Gy1+H}$ and found two soft modes with frequencies of $\omega = -377.74 \text{ cm}^{-1}$ and $\omega = -376.51 \text{ cm}^{-1}$. By displacing the atoms according to the lowest-frequency soft mode, the system relaxes onto

the structure shown on the right in Fig. 2(a), where H and C atoms shift off-plane, but the structure retains an underlying hexagonal lattice, with all threefold C atoms placed at the sites of a honeycomb lattice. The off-plane shifts of the twofold carbons and H atoms are asymmetrical, with one C (H) atom shifting “above” the plane by $\sim 0.21 \text{ \AA}$ (0.71 \AA), and the other two C (H) atoms shifting “below” the plane by $\sim 0.21 \text{ \AA}$ (0.69 \AA) and $\sim 0.16 \text{ \AA}$ (0.52 \AA), respectively. Hence, in this geometry both inversion centers and mirror planes are broken.

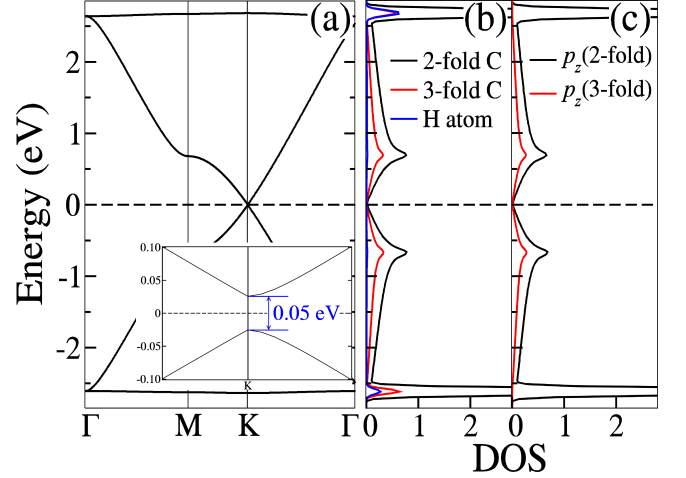


FIG. 5: (a) Band structure of functionalized planar $\alpha\text{Gy2+H}$ along high-symmetry lines in the Brillouin zone. The inset shows gap opening (~ 0.05 eV) on the Dirac point at the Fermi energy, that occurs in the buckled geometry. (b) Black line: partial density of states (PDOS) projected on all basis orbitals of the six twofold C atoms. Red line: PDOS projected on all orbitals of the two threefold C atoms. Blue line: PDOS projected on all orbitals of the six H atoms (c) Black line: PDOS projected on the p_z orbitals of the six twofold C atoms. Red line: PDOS projected on the p_z orbitals of the two threefold C atoms.

The band structure for this buckled $\alpha\text{Gy1+H}$ is shown in Fig. 4(c), where we observe gap openings at the \mathbf{K} -point ranging from 0.16 eV for the Dirac cone above E_f to 0.6 eV for the one below E_f . Gap opening in this case is connected with the breaking of the mirror planes which are present in the planar form. The band structure of $\alpha\text{Gy1+H}$ suggests a poor electronic material with small carrier mobilities associated with the nearly dispersionless band straddling the Fermi level. While stable with respect to Γ -point phonon modes, the buckled $\alpha\text{Gy1+H}$ structure is itself unstable against soft modes in other phonon \vec{q} -vectors, such as the \mathbf{K} and \mathbf{M} points in the BZ, but we do not pursue these lattice instabilities in this report.

We turn now to the more interesting case of the related $\alpha\text{Gy2+H}$ hydrocarbon, with C_8H_6 stoichiometry. In the αGy2 lattice, by bonding one H atom to each twofold C atom, a planar structure that retains the inversion symmetry center in the middle of the chain is

System	Γ	K	M
$\alpha\text{Gy1+H}$ (planar)	-378 , -377	–	–
$\alpha\text{Gy1+H}$ (buckled)	stable	-159	-103
αGy2 (planar)	stable (full)	stable (full)	stable (full)
$\alpha\text{Gy2+H}$ (planar)	-104	stable	stable
$\alpha\text{Gy2+H}$ (buckled)	stable (full)	stable (full)	stable (full)

TABLE I: Frequencies (in cm^{-1}) of unstable phonon modes computed in special \mathbf{k} -points in the Brillouin zone, in pristine and H-functionalized α -graphyne lattices. “Stable” indicates absence of unstable phonon modes at the \mathbf{k} -point indicated. For pristine αGy2 and the buckled $\alpha\text{Gy2+H}$ structures full dispersions along the Γ -K, K-M, and Γ -M high-symmetry lines in the Brillouin zone were computed (indicated by “full” in parenthesis).

formed, as shown on the right in Fig. 2(b). The electronic bands for this planar αGy2 hydrocarbon, shown for a narrower energy interval in Fig. 5(a), display the characteristic Dirac cone at E_f as in pristine αGy2 . The main differences between the band structures of pristine αGy2 and $\alpha\text{Gy2+H}$ in this interval are connected with the saturation of the in-plane p orbitals which move the non-dispersive bands derived from these orbitals away from the Fermi level, making for a “cleaner” electronic structure in an interval of ± 5.0 eV centered on E_f . In this range, we observe only a cone with a Dirac point at E_f , shouldered by a pair of molecular-orbital-like non-dispersive bands, derived mostly from the p_z orbitals of the twofold C atoms, at ± 2.6 eV from E_f .

Regarding lattice stability, the planar $\alpha\text{Gy2+H}$ is unstable against a soft-mode phonon at the Γ point (we found no unstable modes at the K and M points for this structure), and geometry relaxation starting from an initial geometry where atomic positions are displaced according with the soft-phonon mode leads to the geometry shown on the left in Fig. 2(b), where H and twofold C atoms shift out of the plane, resulting in a buckled geometry where some degree of sp^3 bonding is incorporated in the C-C and C-H bonds of the twofold carbons. As a result, we observe the opening of a 0.05 eV gap in the Dirac cone, as shown in the inset in Fig. 5(a).

We observe that in this case the system retains the hexagonal lattice, the inversion centers, and the mirror planes after the out-of-plane relaxation. As in the buckled $\alpha\text{Gy1+H}$, the threefold C atoms occupy the sites of a planar honeycomb lattice. Note that the gap at E_f in this buckled $\alpha\text{Gy2+H}$ structure, due to the mixed hybridization state (mostly sp^2 with some sp^3 character on the twofold-carbon bonds), is one order of magnitude smaller than the gap in the buckled $\alpha\text{Gy1+H}$ and in the planar $\alpha\text{Gy2+O}$ systems (the latter is discussed below).

The full lattice stability of this buckled $\alpha\text{Gy2+H}$ geometry is confirmed by the calculation of the phonon dis-

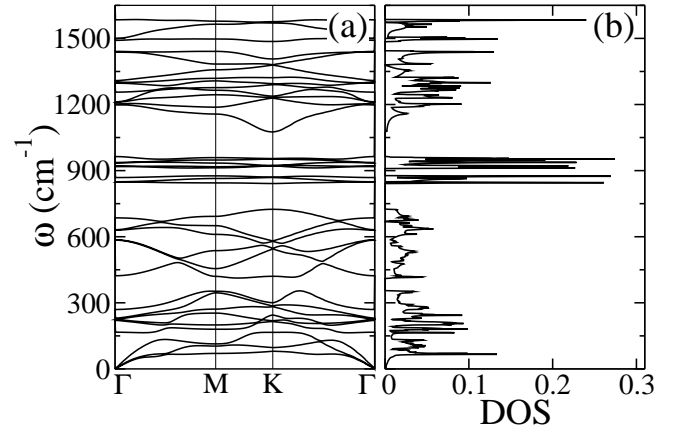


FIG. 6: (a) Phonon spectrum of the buckled $\alpha\text{Gy2+H}$ lattice. Six additional phonon branches, spanning the frequency range of 3082-3108 cm^{-1} , are not shown. (b) Phonon density of states for the buckled $\alpha\text{Gy2+H}$ lattice.

persion and phonon DOS shown in Fig. 6, where no negative frequencies are observed. In the figure, the phonon dispersion is shown along the Γ -K, K-M, Γ -M high-symmetry lines in the BZ. In Table I we summarize the results of our calculations of phonon frequencies in αGy systems.

D. Oxygen functionalization of α -graphyne: electronic structure, symmetry breaking, and gap opening

We switch now to the functionalization of αGy2 with O atoms. Oxygen is known to bind to the graphene sheet in two configurations, depending on the local coverage³⁶. The only stable form at large oxygen coverages is the unzipped configuration, where the O atom is located above the graphene layer, and binds with two C atoms by breaking their mutual C-C bond. Our chemical-bond analysis indicates that a stable oxygenated αG2 form may be expected where the O atoms bind with the twofold carbons through the in-plane p orbitals as in the hydrogenated cases above. In this case, however, one O atom is enough to chemically saturate the pair of twofold C atoms in each chain. We consider thus an αGy2 oxide with C_8O_3 stoichiometry¹⁷.

The resulting planar structure is shown in Fig. 3(c). The cooperative strain mechanism that leads to the unzipped phase of oxygen on graphene³⁷ is not operative in this case, and the O atom makes bonds with the two carbons in the so-called clamped configuration^{36,38}. Unlike in the case of $\alpha\text{G2+H}$, both inversion and mirror symmetries are broken in this case, as shown on the right in Fig. 2, leading to gap opening in the Dirac cone at E_f , as seen in Fig. 7(a). Note that the valence and conduction bands are highly dispersive, indicating low effective masses and hence the possibility of high carrier mobilities

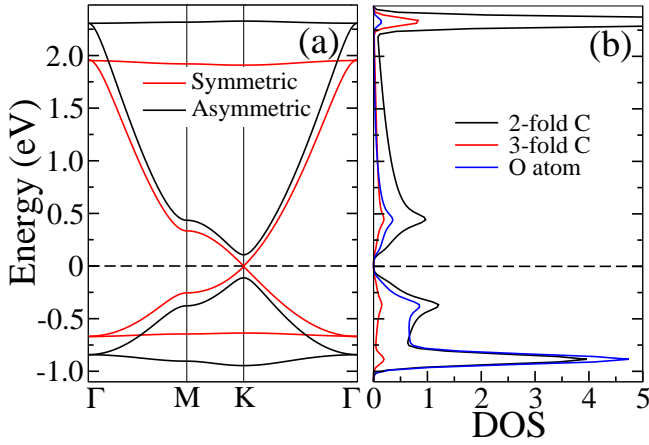


FIG. 7: (a) Band structure of the functionalized planar $\alpha\text{Gy2}+\text{O}$ structure along high-symmetry lines in the Brillouin zone. Black lines: electronic bands for the fully relaxed asymmetric geometry, showing gap opening (0.22 eV) at the Fermi energy. Red lines: electronic bands for a mirror-symmetric geometry, showing no gap opening at the Fermi energy. (b) DOS for the asymmetric structure. Black line: partial density of states (PDOS) projected on all basis orbitals of the six twofold C atoms. Red line: PDOS projected on all orbitals of the two threefold C atoms. Blue line: PDOS projected on all orbitals of the three O atoms.

in this material. This feature, together with the sizeable gap of 0.22 eV, makes this an interesting candidate for a material with a graphene-like gapped dispersion. A full account of the lattice stability of this $\alpha\text{G2}+\text{O}$ will be the subject of a forthcoming study.

IV. SYMMETRY CONSIDERATIONS AND GAP OPENING

Symmetry considerations are in order at this point. The pristine αGy1 lattice, when numerically constrained to a planar honeycomb-like lattice, shows twofold axes at the positions of the twofold carbons (i.e., 2D inversion centers) and mirror planes, hence belongs to the 2D $p6m$ hexagonal-symmetry group. In the relaxed planar geometry of the functionalized $\alpha\text{Gy1}+\text{H}$, the threefold carbons sit on the sites of a perfectly planar honeycomb lattice. However, inversion symmetry is broken in this structure, while the mirror-symmetry planes (intersecting the sheet through the CH bonds) are retained, as can be seen in Fig. 2(a). Thus, $\alpha\text{Gy1}+\text{H}$ belongs to the $p31m$ hexagonal-symmetry group, yet we observe the occurrence of Dirac cones at the **K**-point in the Brillouin zone, as shown in Fig. 4(b).

While inversion symmetry is usually regarded as essential for the occurrence of Dirac cones of electronic states (both the hexagonal-lattice αGy2 and the rectangular-lattice β -graphyne considered in Ref. 12 display inversion centers), even in the absence of inversion symmetry, mirror symmetry ensures the occurrence of Dirac cones in

the electronic structure of the planar $\alpha\text{Gy1}+\text{H}$ system, as shown in Fig. 4(b). Mirror-symmetry breaking in the buckled $\alpha\text{Gy1}+\text{H}$ lattice reduces the symmetry of this system to the $p3$ hexagonal-symmetry group and leads to gap opening in the Dirac cones at the **K**-point.

Note that, from the point of view of the transformation of the p_z orbitals under these symmetries, the mirror planes and inversion centers differ only by a phase. In a related result, in Ref. 39 a mirror symmetry was shown to be connected with the occurrence of Dirac cones on the electronic states associated with grain boundaries in graphene.

In the case of αGy2 , both the planar and buckled forms of $\alpha\text{Gy2}+\text{H}$ belong to the $p6m$ symmetry group and gap opening in the buckled lattice is not connected with symmetry breaking, as discussed above.

The $\alpha\text{Gy2}+\text{O}$ case is similar to $\alpha\text{Gy1}+\text{H}$: a mirror-symmetry-constrained planar lattice displays mirror symmetry planes and no inversion centers, thus belonging to the $p31m$ group, and gapless Dirac cones appear in its electronic spectrum [Fig. 7(a)], while in the unconstrained lattice mirror symmetry is broken, the overall symmetry is reduced to the $p3$ group, and we observe gap openings at the Dirac points.

A. Massive Dirac-fermion nature of carriers in functionalized α -graphynes

Let us focus now on the Dirac-fermion nature of the electronic carriers in these α -graphyne systems. That the carriers in the $\alpha\text{Gy2}+\text{O}$ lattice can be described as massive Dirac fermions is confirmed by the excellent fittings we obtain for the dependence of the energy of the Dirac-like bands to the relativistic dispersion relation for massive fermions:

$$E^2(\vec{k}) = \hbar^2 k^2 v_F^2 + m^2 v_F^4; \quad (1)$$

where v_F and m are, respectively, the effective “speed of light” and mass of the Dirac-fermions. A natural choice is to set the rest-energy term to $m^2 v_F^4 = (E_g/2)^2$, where E_g is the gap that opens at the Dirac point. With that choice, by fitting the energy bands of this system to Eq. 1, we obtain the carrier velocities in Table II. Included in the table are the electron and holes velocities along the **M-K** and **K-Γ** directions in the BZ. We remark that v_F values in Table II show that the bands of $\alpha\text{Gy2}+\text{O}$ are essentially isotropic with a rather small ($\sim 5\text{-}6\%$) electron-hole asymmetry.

The opposite is true in the case of the buckled $\alpha\text{Gy2}+\text{H}$ lattice. The dispersion relation near the Fermi energy is strongly anisotropic, displaying a linear behavior along the **M-K** direction and a quadratic one along the **K-Γ** direction, as can be seen in the inset in Fig. 5. Hence, carriers in this system should behave as massless Dirac fermions along the **M-K** line and as massive fermions along the **K-Γ** line.

Also included in Table II are the Fermi velocities for the massless Dirac fermions of pristine αGy2 and the planar $\alpha\text{Gy2+H}$ geometry, obtained from the fitting of the corresponding gapless dispersion relations to $E(\vec{k}) = \hbar k v_F$.

	v_F^e		v_F^h		m		t_{eff}
System	M-K	K-Γ	M-K	K-Γ	M-K	K-Γ	
αGy2	0.671	0.696	0.667	0.692	0	0	0.75
$\alpha\text{Gy2+H}$ (planar)	0.568	0.598	0.568	0.595	0	0	0.68
$\alpha\text{Gy2+H}$ (buckled)	0.568	0.611	0.561	0.611	0	0.01	0.71
$\alpha\text{Gy2+O}$ (planar)	0.349	0.349	0.329	0.333	0.18	0.18	0.41

TABLE II: Carrier velocities v_F^e (electrons) and v_F^h (holes), in units of 10^6 m/s, along the **M-K** and **K- Γ** directions in the Brillouin zone, and values of carrier mass m , in units of bare electron mass (m_{bare}), in pristine and functionalized αGy2 lattices, from fittings to relativistic dispersion relations for massless and massive Dirac fermions. Effective hopping t_{eff} (in eV), from tight-binding model.

From Table II, we observe that a sizeable renormalization of the Fermi velocity takes place in the pristine αGy2 lattice ($v_F = 0.68 \times 10^6$ m/s), when compared with graphene ($v_F = 1.00 \times 10^6$ m/s). In a simple orthogonal first-neighbor tight-binding (TB) picture, the Fermi velocity of the Dirac fermions is given by $v_F = \sqrt{3}ta_0/2\hbar$, where t is the hopping parameter and a_0 is the lattice constant.

An effective hopping parameter for each of these systems can be defined from the gap Δ_M between the two van Hove singularities at the **M**-point in the BZ, i.e., $t_{eff} = \Delta_M/2$, as given by this simple TB model. The values of the t_{eff} in each case, obtained from this prescription, are also included in Table II. We observe that the renormalization of v_F in these αGy2 lattices is connected with a strong reduction of the effective hopping parameter, from ~ 3 eV in graphene to 0.41-0.75 eV in α -graphynes.

V. CONCLUSIONS

In conclusion, through *ab initio* calculations we investigate the electronic structure and the lattice stability of pristine and functionalized (with either H or O atoms) α -graphyne systems with one (αGy1) and two (αGy2) atoms along the twofold-carbon chains. We identify their lattice instabilities, connected with soft-phonon modes, and describe two mechanisms leading to gap opening in

the Dirac-fermion electronic spectrum of these systems: symmetry-breaking connected with the lattice instabilities and partial incorporation of an sp^3 character in the bonding network of the hydrogenated $\alpha\text{Gy2+H}$, where the fully-lattice-stable buckled geometry retains the symmetries of the parent pristine αGy2 .

More specifically, our calculations indicate that a 2D lattice of pristine αGy2 is fully stable, displaying no soft phonon modes, while its planar hydrogenated counterpart $\alpha\text{Gy2+H}$ is unstable against a Γ -point soft-phonon mode. The instability drives the system to a fully-stable buckled geometry, where twofold C atoms and saturating H atoms shift off the plane of the threefold C atoms. In the case of αGy1 , while a pristine 2D lattice is found to be unstable due to chemical-bond frustration, a planar $\alpha\text{Gy1+H}$ geometry is chemically stabilized by saturation of in plane p orbitals that inhibits the formation of the destabilizing π bonds. The planar $\alpha\text{Gy1+H}$ lacks inversion symmetry but retains mirror planes that are found to suffice for the occurrence of gapless Dirac cones in the electronic dispersion of this system. Mirror-symmetry breaking and concurrent gap openings in the Dirac cones take place in a buckled $\alpha\text{Gy1+H}$ lattice.

In the case of a planar $\alpha\text{Gy2+O}$ system, a single O atom bind asymmetrically to the two C atoms in the twofold chain, breaking inversion and mirror symmetries, and leading to the opening of a sizeable gap of ~ 0.22 eV in the Dirac cone at the Fermi level.

Finally, in this study we also analyze the gapless and gapped Dirac cones of the αGy2 , $\alpha\text{Gy2+H}$, and $\alpha\text{Gy2+O}$ systems from the perspective of the dispersion relations for massless and massive free Dirac fermions. We find that mirror-symmetry breaking operates as a Dirac-fermion mass-generation mechanism in $\alpha\text{Gy2+O}$, leading to gap opening and to isotropic electronic dispersions with a rather small electron-hole asymmetry. In $\alpha\text{Gy2+H}$, carriers display a remarkable anisotropy, acting as massless fermions along the **M-K** line in the Brillouin zone and as massive fermions along the **Γ -K** line. Renormalization of carrier velocities αGy2 lattices is found to be due to a strong reduction of the effective hopping parameter, when compared with graphene.

Acknowledgement

We acknowledge funding from Brazilian agencies CNPq, FAPEMIG, Capes, and Instituto Nacional de Cincia e Tecnologia (INCT) em Nanomateriais de Carbono - MCT.

¹ K. S. Novoselov, A. K. Geim, S. V. Morozov, D. Jiang, Y. Zhang, S. V. Dubonos, I. V. Grigorieva, and A. A. Firsov, Science **306**, 666 (2004).

² P. Sutter, J.-I. Flege, and E. Sutter, Nature Materials **7**, 406 (2008).

³ X. Li, W. Cai, J. An, S. Kim, J. Nah, D. Yang, R. Piner,

- A. Velamakanni, I. Jung, E. Tutuc, et al., *Science* **324**, 1312 (2009).
- ⁴ A. H. Castro Neto, F. Guinea, N. M. R. Peres, K. S. Novoselov, and A. K. Geim, *Rev. Mod. Phys.* **81**, 109 (2009), URL <http://link.aps.org/doi/10.1103/RevModPhys.81.109>.
 - ⁵ A. K. Geim and K. S. Novoselov, *Nat Mater* **6**, 183 (2007).
 - ⁶ J. Ribeiro-Soares and M. Dresselhaus, *Brazilian Journal of Physics* pp. 1–5 (2013).
 - ⁷ L. Kou, B. Yan, F. Hu, S.-C. Wu, T. O. Wehling, C. Felser, C. Chen, and T. Frauenheim, *Nano Letters* **13**, 6251 (2013), <http://pubs.acs.org/doi/pdf/10.1021/nl4037214>, URL <http://pubs.acs.org/doi/abs/10.1021/nl4037214>.
 - ⁸ L. Chen, C.-C. Liu, B. Feng, X. He, P. Cheng, Z. Ding, S. Meng, Y. Yao, and K. Wu, *Phys. Rev. Lett.* **109**, 056804 (2012), URL <http://link.aps.org/doi/10.1103/PhysRevLett.109.056804>.
 - ⁹ Y. Shi, C. Hamsen, X. Jia, K. K. Kim, A. Reina, M. Hofmann, A. L. Hsu, K. Zhang, H. Li, Z.-Y. Juang, et al., *Nano Letters* **10**, 4134 (2010).
 - ¹⁰ P. Joensen, R. Frindt, and S. Morrison, *Materials Research Bulletin* **21**, 457 (1986).
 - ¹¹ B. G. Kim and H. J. Choi, *Phys. Rev. B* **86**, 115435 (2012).
 - ¹² D. Malko, C. Neiss, F. Viñes, and A. Görling, *Phys. Rev. Lett.* **108**, 086804 (2012), URL <http://link.aps.org/doi/10.1103/PhysRevLett.108.086804>.
 - ¹³ F. Diederich, *Nature* **369**, 199 (1994), URL <http://dx.doi.org/10.1038/369199a0>.
 - ¹⁴ J. M. Kehoe, J. H. Kiley, J. J. English, C. A. Johnson, R. C. Petersen, and M. M. Haley, *Organic Letters* **2**, 969 (2000).
 - ¹⁵ F. Diederich and M. Kivala, *Advanced Materials* **22**, 803 (2010), ISSN 1521-4095, URL <http://dx.doi.org/10.1002/adma.200902623>.
 - ¹⁶ D. Malko, C. Neiss, and A. Görling, *Phys. Rev. B* **86**, 045443 (2012), URL <http://link.aps.org/doi/10.1103/PhysRevB.86.045443>.
 - ¹⁷ B. Kang, H. Liu, and J. Y. Lee, *Phys. Chem. Chem. Phys.* **16**, 974 (2014), URL <http://dx.doi.org/10.1039/C3CP53237B>.
 - ¹⁸ A. N. Enyashin and A. L. Ivanovskii, *physica status solidi (b)* **248**, 1879 (2011), ISSN 1521-3951, URL <http://dx.doi.org/10.1002/pssb.201046583>.
 - ¹⁹ J. Soler, E. Artacho, J. Gale, A. García, J. Junquera, P. Ordejón, and D. Sánchez-Portal, *Journal of Physics: Condensed Matter* **14**, 2745 (2002).
 - ²⁰ H. J. Monkhorst and J. D. Pack, *Phys. Rev. B* **13**, 5188 (1976), URL <http://link.aps.org/doi/10.1103/PhysRevB.13.5188>.
 - ²¹ D. Hamann, M. Schlüter, and C. Chiang, *Physical Review Letters* **43**, 1494 (1979).
 - ²² L. Kleinman and D. M. Bylander, *Phys. Rev. Lett.* **48**, 1425 (1982), URL <http://link.aps.org/doi/10.1103/PhysRevLett.48.1425>.
 - ²³ G. Román-Pérez and J. Soler, *Physical review letters* **103**, 96102 (2009).
 - ²⁴ M. Dion, H. Rydberg, E. Schröder, D. C. Langreth, and B. I. Lundqvist, *Phys. Rev. Lett.* **92**, 246401 (2004), URL <http://link.aps.org/doi/10.1103/PhysRevLett.92.246401>.
 - ²⁵ J. Perdew, K. Burke, and M. Ernzerhof, *Physical review letters* **77**, 3865 (1996).
 - ²⁶ S. Baroni, S. de Gironcoli, A. Dal Corso, and P. Giannozzi, *Rev. Mod. Phys.* **73**, 515 (2001), URL <http://link.aps.org/doi/10.1103/RevModPhys.73.515>.
 - ²⁷ P. Giannozzi, S. Baroni, N. Bonini, M. Calandra, R. Car, C. Cavazzoni, D. Ceresoli, G. L. Chiarotti, M. Cococcioni, I. Dabo, et al., *Journal of Physics: Condensed Matter* **21**, 395502 (2009), URL <http://stacks.iop.org/0953-8984/21/i=39/a=395502>.
 - ²⁸ A. M. Rappe, K. M. Rabe, E. Kaxiras, and J. D. Joannopoulos, *Phys. Rev. B* **41**, 1227 (1990), URL <http://link.aps.org/doi/10.1103/PhysRevB.41.1227>.
 - ²⁹ D. Vanderbilt, *Phys. Rev. B* **41**, 7892 (1990), URL <http://link.aps.org/doi/10.1103/PhysRevB.41.7892>.
 - ³⁰ N. Marzari, D. Vanderbilt, A. De Vita, and M. C. Payne, *Phys. Rev. Lett.* **82**, 3296 (1999), URL <http://link.aps.org/doi/10.1103/PhysRevLett.82.3296>.
 - ³¹ G. Trinquier and J. P. Malrieu, *Journal of the American Chemical Society* **109**, 5303 (1987), <http://pubs.acs.org/doi/pdf/10.1021/ja00252a002>, URL <http://pubs.acs.org/doi/abs/10.1021/ja00252a002>.
 - ³² Y. Ohshima, S. Yamamoto, M. Nakata, and K. Kuchitsu, *The Journal of Physical Chemistry* **91**, 4696 (1987), <http://pubs.acs.org/doi/pdf/10.1021/j100302a014>, URL <http://pubs.acs.org/doi/abs/10.1021/j100302a014>.
 - ³³ V. O. Özçelik and S. Ciraci, *The Journal of Physical Chemistry C* **117**, 2175 (2013), <http://pubs.acs.org/doi/pdf/10.1021/jp3111869>, URL <http://pubs.acs.org/doi/abs/10.1021/jp3111869>.
 - ³⁴ B. G. Kim and H. J. Choi, *Phys. Rev. B* **86**, 115435 (2012), URL <http://link.aps.org/doi/10.1103/PhysRevB.86.115435>.
 - ³⁵ J.-M. Ducr, C. Lepetit, and R. Chauvin, *The Journal of Physical Chemistry C* **117**, 21671 (2013), <http://pubs.acs.org/doi/pdf/10.1021/jp4067795>, URL <http://pubs.acs.org/doi/abs/10.1021/jp4067795>.
 - ³⁶ Z. Xu and K. Xue, *Nanotechnology* **21**, 045704 (2010).
 - ³⁷ J.-L. Li, K. N. Kudin, M. J. McAllister, R. K. Prud'homme, I. A. Aksay, and R. Car, *Phys. Rev. Lett.* **96**, 176101 (2006), URL <http://link.aps.org/doi/10.1103/PhysRevLett.96.176101>.
 - ³⁸ J.-A. Yan, L. Xian, and M. Y. Chou, *Phys. Rev. Lett.* **103**, 086802 (2009), URL <http://link.aps.org/doi/10.1103/PhysRevLett.103.086802>.
 - ³⁹ J. da Silva Araújo and R. W. Nunes, *Phys. Rev. B* **81**, 073408 (2010), URL <http://link.aps.org/doi/10.1103/PhysRevB.81.073408>.